

High-order expansions of multi-revolution elliptic Halo orbits in the elliptic restricted three-body problem

Xiaoyan Leng^{1,2} and Hanlun Lei^{1,2*}

¹School of Astronomy and Space Science, Nanjing University, Nanjing, 210023, China.

²Key Laboratory of Modern Astronomy and Astrophysics in Ministry of Education, Nanjing University, Nanjing, 210023, China.

*Corresponding author(s). E-mail(s): leihl@nju.edu.cn;

Abstract

Multi-revolution elliptic Halo (ME-Halo) orbits are a special class of symmetric and periodic solutions within the framework of the elliptic restricted three-body problem (ERTBP). During a single period, an M:N ME-Halo orbit completes M revolutions around a libration point and the primaries revolve N times around each other. Owing to the repeated configurations, ME-Halo orbits hold great promise as nominal trajectories for space mission design. However, a major challenge associated with ME-Halo orbits lies in their mathematical description. To this end, we propose a novel method to derive high-order analytical expansions of ME-Halo orbits in the ERTBP by introducing two correction terms into the equations of motion in the y - and z -directions. Specifically, both the coordinate variables and correction terms are expanded as power series in terms of the primary eccentricity, the in-plane amplitude, and the out-of-plane amplitude. High-order approximations are constructed using a perturbation method, and their accuracy is validated through numerical analysis. Due to the inherent symmetry, ME-Halo orbits can be classified into four distinct families: southern/northern and periapsis/apoapsis groups. The analytical approximations developed in this study not only provide high-accuracy initial guesses for the numerical computation of ME-Halo orbits, but also offer new insights into the dynamical environment near collinear libration points in the ERTBP, thereby advancing practical applications in mission design.

Keywords: Perturbation method, Multi-revolution elliptic Halo orbits, Double resonance

1 Introduction

The three-body problem remains one of the most enduring and fundamental challenges in celestial mechanics. In particular, in the circular restricted three-body problem (CRTBP) there are five equilibrium points, at which the gravitational and centrifugal forces are precisely balanced. These points are of particular interest for space missions ([Bernelli Zazzera et al. 2004](#); [Masdemont 2005](#); [Peng and Xu 2015a](#); [Neelakantan and](#)

Ramanan 2022; Chujo 2024; Burattini et al. 2024; Conti and Circi 2025; Sanaga and Howell 2025; Gao et al. 2025; Yamaguchi et al. 2025).

Regarding the issue of CRTBP, Szebehely (1967) provided a comprehensive review about analytical and numerical methods to investigate the dynamics near libration points. Following this methodological framework, Farquhar and Kamel (1973) employed the Lindstedt–Poincaré (L–P) method to explore quasi-periodic orbits near the Earth–Moon libration points, successfully revealing the existence of Halo orbits. Richardson (1980) further applied the L–P method to derive a third-order analytical solution of Halo orbits, which has been widely used to provide initial guesses for computing Halo orbits. Based on partial normalization via the Lie series method, Jorba and Masdemont (1999) reduced the dynamics near the equilibrium points to the center manifold, where the dynamical behavior was typically analyzed by means of Poincaré sections. The L–P technique was adopted to formulate high-order expansions of center manifolds, including Lissajous and Halo orbits. This topic was extended by Masdemont (2005) to invariant manifolds, enabling accurate modeling of motion near libration points and supporting practical applications such as low-energy transfers, station-keeping, and trajectory design between L_1 and L_2 . In addition, it shows that the Koopman Operator can be used to formulate analytical solutions for Lyapunov and Halo orbits (Servadio et al. 2023).

Analytical progress has been made in understanding the bifurcation mechanisms of Halo orbits. By constructing a normal form adapted to the synchronous resonance, and introducing a detuning parameter to characterize the frequency deviation, Cecconari et al. (2016) derived energy thresholds for the onset of Halo orbit bifurcations under arbitrary mass ratios. Luo et al. (2020) obtained analytical forms of normalized Hamiltonian functions, and derived the formula for the bifurcation energy. Furthermore, they provided the analytical solutions of Lissajous and halo orbits through an inverse transformation. Recently, Lin and Chiba (2025) proposed a generalized dynamical framework by incorporating a coupling coefficient, which facilitates the unified description of Lissajous, Halo, and quasi-Halo orbits.

While the CRTBP remains applicable in certain contexts, its limitations are well recognized. In particular, Parker and Anderson (2014) identified that the non-zero eccentricity of the primaries' orbits may lead to deviations from orbital periodicity. To this end, the elliptic restricted three-body problem (ERTBP) provides a more accurate representation of spacecraft dynamics. Within the framework of ERTBP, Heppenheimer (1973) investigated the out-of-plane motion near the libration points and analyzed the influence of amplitude and eccentricity upon the orbital periods. From an analytical viewpoint, Hou and Liu (2011) developed high-order solutions for Lissajous and Halo orbits, and classified three types of symmetric periodic orbits. About the same topic, Lei et al. (2013) extended to high-order expansions of invariant manifolds around collinear libration points in the ERTBP. Paez and Guzzo (2022) advanced the theory of Halo orbits in the ERTBP by developing high-order approximations of quasi-periodic orbits and their associated invariant manifolds, employing a resonant Floquet–Birkhoff normal form. Recently, Celletti et al. (2024) applied the normalization technique to the ERTBP, providing analytical solutions for Lyapunov and Halo orbits near the libration points, along with expressions for the bifurcation energies.

Due to the periodic perturbations introduced by the orbital eccentricity of the secondary body, periodic orbits in the CRTBP generally lose strict periodicity when extended to the ERTBP, evolving into quasi-periodic trajectories. Nevertheless, strictly periodic orbits do exist within the framework of ERTBP. As early as 1920, [Moulton \(1920\)](#) proposed a geometric criterion for strong periodicity in the ERTBP. Later, [Sarris \(1989\)](#) demonstrated that, unlike in the CRTBP—where orbital periods can assume arbitrary values—only integer multiples of 2π are permitted in the ERTBP. Building upon these foundational insights, [Campagnola et al. \(2008\)](#) coined the term ‘elliptic Halo orbits’ to describe the ERTBP counterparts of CRTBP Halo orbits and computed them using eccentricity-based numerical continuation with CRTBP Halo orbits as initial guesses. [Peng and Xu \(2015b\)](#) further referred to these trajectories as ‘multi-revolution elliptic Halo (ME-Halo) orbits’¹ and employed the technique of arc-length continuation to avoid singularities associated with single-parameter continuation methods. Using the variation of constants, [Asano et al. \(2015\)](#) formulated a second-order approximation for ME-Halo orbits around collinear libration points. In a systematic study, [Ferrari and Lavagna \(2018\)](#) extended Lyapunov, vertical Lyapunov, and Halo orbits from the CRTBP to the ERTBP, obtaining single-, double-, triple-, and quadruple-revolution Halo orbits. [Neelakantan and Ramanan \(2021\)](#) introduced a differential evolution-based method for designing multi-revolution periodic orbits, enabling the computation of multi-revolution Lyapunov and Halo orbits. For solar sails in the Sun–Earth ERTBP, [Huang et al. \(2020\)](#) constructed ME-Halo orbits and identified bifurcations based on stability analysis. Periodic orbits have been investigated in [Zheng and Zhao \(2024\)](#) by numerically continuing models from the CRTBP to the ERTBP. Applications of ME-Halo orbits in mission design have been widely discussed ([Peng and Xu 2015a,c; Peng et al. 2017; Peng and Bai 2018; Neelakantan and Ramanan 2022](#)).

From the aforementioned studies, we can see that numerical methods have thus far been the primary means for generating ME-Halo orbits within the framework of ERTBP. However, a key challenge of these approaches lies in their sensitivity to initial conditions. Initial guesses derived from Halo orbits in the CRTBP typically require successive corrections through eccentricity continuation and multi-shooting methods, thereby increasing the computational complexity([Campagnola et al. 2008; Peng and Xu 2015b; Ferrari and Lavagna 2018](#)). This raises a fundamental question: is it possible to develop an analytical approximation for ME-Halo orbits directly within the ERTBP framework? The primary objective of this study is to answer this question. We hope to construct an analytical approximation that not only provides high-accuracy initial guesses for the numerical construction of ME-Halo orbits but also offers new insights into the dynamical behavior near collinear libration points, thereby advancing both theoretical understanding and practical applications.

The remainder of this paper is organized as follows. In Section 2, we briefly introduce the dynamical model. Section 3 shows the details of formulating high-order expansions of ME-Halo orbits in the framework of ERTBP. Analytical results of ME-Halo orbits are given in Section 4, and numerical explorations are made in Section 5. At last, the main conclusion is summarized in Section 6.

¹We adopt the terminology ‘multi-revolution elliptic Halo orbits’ (ME-Halo orbits for short) in this study.

2 Elliptic restricted three-body problem

The elliptic restricted three-body problem (ERTBP) studies the motion of a massless third body, denoted by P_3 , under the gravitational field of two primaries, denoted by P_1 and P_2 . Let us denote the mass of the third body as m , the masses of the primary bodies as m_1 and m_2 . Without loss of generality, we assume $m_1 > m_2$. In the test-particle limit, it holds $m \ll m_2 < m_1$, showing that P_3 has negligible influence on the motion of the primaries. Thus, the primaries move around their barycenter in Keplerian orbits with eccentricity of e . In particular, when the eccentricity is $e = 0$, the ERTBP reduces to the circular restricted three-body problem (CRTBP).

Usually, the motion of P_3 is described in a barycentric synodic coordinate system, where the X -axis points from P_1 toward P_2 , the Z -axis is aligned with the angular momentum vector of the primaries, and the Y -axis is chosen to complete the right-handed rule. For convenience, the following system of units is used: the instantaneous distance between the primaries is taken as the unit of length, the total mass of primaries as the unit of mass, and the orbital period divided by 2π as the time unit. Under the normalized system of units, both the mean motion of the primaries and the universal gravitational constant become unity. In addition, the secondary P_2 with normalized mass of $\mu = m_2/(m_1 + m_2)$ is located at $(1 - \mu, 0, 0)$, and the primary P_1 with normalized mass of $1 - \mu$ is located at $(-\mu, 0, 0)$.

In the ERTBP, the equations of motion for the test particle P_3 can be written as (Szebehely 1967)

$$X'' - 2Y' = \frac{1}{1 + e \cos f} \frac{\partial \Omega}{\partial X}, \quad Y'' + 2X' = \frac{1}{1 + e \cos f} \frac{\partial \Omega}{\partial Y}, \quad Z'' = \frac{1}{1 + e \cos f} \frac{\partial \Omega}{\partial Z}, \quad (1)$$

where the effective potential is given by

$$\Omega = \frac{1}{2} [X^2 + Y^2 + Z^2 + \mu(1 - \mu)] + \frac{1 - \mu}{R_1} + \frac{\mu}{R_2} \quad (2)$$

with R_1 and R_2 being the distances of P_3 from P_1 and P_2 , respectively. In Eq. (1), f is the true anomaly of the primary orbit and the prime symbol denotes the derivative with respect to the true anomaly. With the X component as an example, it reads

$$X' = \frac{dX}{df}, \quad X'' = \frac{d^2X}{df^2}. \quad (3)$$

In the ERTBP, there are five equilibrium points (Szebehely 1967), three of them are located on the X -axis, called collinear libration points, and the remaining two constitute equilateral triangles with the primaries, called triangular libration points. The focus of this work is to study the motion around collinear libration points. To this end, it is required to first move the origin of coordinate system to the libration point of interest, and then take the instantaneous distance between the considered libration point and its nearest primary γ_i as the new unit of length. The coordinate transformation between the original barycentric synodic frame and the L_i -centered frame can be realized by

$$X = \gamma_i (x \mp 1) + 1 - \mu, \quad Y = \gamma_i y, \quad Z = \gamma_i z, \quad i = 1, 2 \quad (4)$$

where the upper sign refers to the L_1 point and the lower one refers to the L_2 point (L_3 is not considered in this study). In the L_i -centered synodic system, the equations of motion can be organized as follows (Hou and Liu 2011; Lei et al. 2013):

$$\begin{aligned} x'' - 2y' &= \sum_{i \geq 0} (-e)^i \cos^i f (1 + 2c_2)x + \sum_{i \geq 0} \sum_{n \geq 2} (-e)^i \cos^i f c_{n+1}(n+1)T_n, \\ y'' + 2x' &= \sum_{i \geq 0} (-e)^i \cos^i f (1 - c_2)y + \sum_{i \geq 0} \sum_{n \geq 2} (-e)^i \cos^i f c_{n+1}y R_{n-1}, \\ z'' + c_2z &= \sum_{i \geq 1} (-e)^i \cos^i f (1 - c_2)z + \sum_{i \geq 0} \sum_{n \geq 2} (-e)^i \cos^i f c_{n+1}z R_{n-1}. \end{aligned} \quad (5)$$

In the above equations, c_n is determined by the mass parameter μ , given by

$$c_n = \frac{1}{\gamma_i^3} [(\pm 1)^n \mu + (-1)^n \frac{(1 - \mu) \gamma_i^{n+1}}{(1 \mp \gamma_i)^{n+1}}], \quad i = 1, 2 \quad (6)$$

where the upper sign is for the L_1 point and the lower sign is for the L_2 point. Additionally, T_n and R_{n-1} are defined by (Jorba and Masdemont 1999)

$$T_n = \rho^n P_n\left(\frac{x}{\rho}\right), \quad R_{n-1} = \frac{1}{y} \frac{\partial T_{n+1}}{\partial y} = \frac{1}{z} \frac{\partial T_{n+1}}{\partial z}, \quad (7)$$

where $P_n(\cdot)$ is the Legendre polynomial and ρ is the distance $\rho = \sqrt{x^2 + y^2 + z^2}$. In particular, T_n and R_n are homogeneous polynomials of degree n of coordinates, computed recursively by (Jorba and Masdemont 1999)

$$\begin{aligned} T_n &= \frac{2n-1}{n} x T_{n-1} - \frac{n-1}{n} (x^2 + y^2 + z^2) T_{n-2}, \\ R_n &= \frac{2n+3}{n+2} x R_{n-1} - \frac{2n+2}{n+2} T_n - \frac{n+1}{n+2} (x^2 + y^2 + z^2) R_{n-2}, \end{aligned} \quad (8)$$

starting with $T_0 = 1$, $T_1 = x$, $R_0 = -1$, and $R_1 = -3x$.

3 Analytic construction of ME-Halo orbits

In the ERTBP, the perturbation introduced by the orbital eccentricity e typically causes Halo orbits to exhibit quasi-periodic behavior. However, when the motion frequency of a Halo orbit forms a simple integer ratio with the system's forced frequency, resonance effects can make the orbit become periodic. According to the definition given by Peng and Xu (2015b), a periodic orbit is defined as the $M:N$ ME-Halo orbit if its period T_E is an integer multiple of the system's fundamental period 2π ($T_E = N \cdot 2\pi$), and also an integer multiple of the corresponding Halo orbit period T_C in the CRTBP ($T_E = M \cdot T_C$)². Without loss of generality, in this section we take M2N1 ME-Halo orbits as an example to discuss the construction of high-order series expansions.

²The period of CRTBP Halo orbit is $T_C = 2\pi/\omega = 2\pi/\nu$, where ω and ν are the in-plane and out-of-plane motion frequencies, respectively.

3.1 The basic idea

It is known that Halo orbits in the CRTBP are a type of three-dimension periodic orbits, which are bifurcated from the family of planar Lyapunov orbits. Thus, the emergence of Halo orbits is due to the frequency degeneracy condition, where the frequency of in-plane motion ω is exactly equal to that of out-of-plane motion ν . To realize the Halo orbit condition of $\omega = \nu$ in the CRTBP, [Richardson \(1980\)](#) and [Jorba and Masdemont \(1999\)](#) introduced a correction term Δz in the z -direction equation of motion and developed high-order expansions of Halo orbits by means of L–P method. Similarly, [Hou and Liu \(2011\)](#) and [Lei et al. \(2013\)](#) introduced the correction term Δz in the z -direction equation of motion to reach the condition of $\omega = \nu$ in the ERTBP. Particularly, here Δ must also be expanded as a power series of in-plane and out-of-plane amplitudes, where the coefficients are solved iteratively via the L–P method. The correction condition of $\Delta = 0$ indicates that in-plane and out-of-plane amplitudes (usually denoted by α and β) of Halo orbits are no longer independent. Thus, we can see that the degeneracy condition of fundamental frequencies ($\omega = \nu$) is realized by introduction of $\Delta = 0$.

Generally, Halo orbits with $\omega = \nu$ in the ERTBP are no longer periodic due to the existence of an additional forced frequency caused by the primary's eccentricity. Only when the forced frequency and the in-plane (or out-of-plane) frequency are still commensurable, the Halo orbits may become periodic. The resulting periodic Halo orbits are termed ME-Halo orbits. Thus, we can interpret ME-Halo orbits as a class of orbits embedded within double resonance structures. In particular, one resonance involves a commensurability between two natural frequencies, whereas the other involves a commensurability between a natural and a forced frequency.

Inspired by the construction of Halo orbits in the CRTBP, we propose a high-order expansion approach for ME-Halo orbits by introducing two correction terms: (a) the first correction term, denoted as $\Delta_1 y$, is added to the y -direction equation of motion³ to ensure that the forced frequency is commensurable with either the in-plane or out-of-plane natural frequency; and (b) the second correction term, denoted as $\Delta_2 z$, is introduced in the z -direction equation of motion to enforce a 1:1 resonance between the in-plane and out-of-plane motions ($\omega = \nu$).

The equations of motion with correction terms are written as

$$\begin{aligned} x'' - 2y' &= \sum_{i \geq 0} (-e)^i \cos^i f (1 + 2c_2)x + \sum_{i \geq 0} \sum_{n \geq 2} (-e)^i \cos^i f c_{n+1}(n+1)T_n, \\ y'' + 2x' &= \sum_{i \geq 0} (-e)^i \cos^i f (1 - c_2)y + \sum_{i \geq 0} \sum_{n \geq 2} (-e)^i \cos^i f c_{n+1}y R_{n-1} + \Delta_1 y, \\ z'' + c_2 z &= \sum_{i \geq 1} (-e)^i \cos^i f (1 - c_2)z + \sum_{i \geq 0} \sum_{n \geq 2} (-e)^i \cos^i f c_{n+1}z R_{n-1} + \Delta_2 z. \end{aligned} \quad (9)$$

³It is worth noting that applying the same method to introduce $\Delta_1 x$ for correction in the x -direction yields parameter values that deviate significantly from those obtained through correction in the y -direction. Moreover, when the analytical solution derived from the x -direction correction is used as the initial condition for numerical integration, the resulting trajectory exhibits divergence. The underlying cause of this pronounced discrepancy in the x -direction correction remains unclear and warrants further investigation.

The invariance of equations of motion requires the correction conditions of $\Delta_1 = 0$ and $\Delta_2 = 0$, leading to implicit relationships among the eccentricity e , in-plane amplitude α and out-of-plane amplitude β .

3.2 Third-order analytical solution

Perturbation method is employed to derive third-order analytical solutions for ME-Halo orbits through a recursive process, starting from the linear solution (Lei 2024). It should be noted that the third-order solution represents the lowest order at which nonlinear corrections associated with ME-Halo resonances emerge, just like the third-order solution of Halo orbits in the CRTBP (Richardson 1980). To formulate third-order solution, the equations of motion are truncated up to third order with respect to the variables (e, x, y, z) as follows:

$$\begin{aligned}
x'' - 2y' - (1 + 2c_2)x &= \frac{3}{2}c_3(2x^2 - y^2 - z^2) - (1 + 2c_2)ex \cos f \\
&\quad + \frac{1}{2}(1 + 2c_2)(1 + \cos 2f)e^2x - \frac{3}{2}c_3(2ex^2 - ey^2 - ez^2) \cos f \\
&\quad + 2c_4x(2x^2 - 3y^2 - 3z^2), \\
y'' + 2x' - (1 - c_2)y &= -3c_3xy - (1 - c_2)ey \cos f \\
&\quad + \frac{1}{2}(1 - c_2)(1 + \cos 2f)e^2y + 3c_3exy \cos f \\
&\quad - \frac{3}{2}c_4y(4x^2 - y^2 - z^2) + \Delta_1y, \\
z'' + c_2z &= -3c_3xz - (1 - c_2)ez \cos f + \frac{1}{2}(1 - c_2)(1 + \cos 2f)e^2z \\
&\quad + 3c_3exz \cos f - \frac{3}{2}c_4z(4x^2 - y^2 - z^2) + \Delta_2z.
\end{aligned} \tag{10}$$

Up to the third order in terms of (e, x, y, z) , the coordinates (x, y, z) as well as the correction terms (Δ_1 and Δ_2) are expanded as follows:

$$\begin{aligned}
x &= x_1 + x_2 + x_3, \\
y &= y_1 + y_2 + y_3, \\
z &= z_1 + z_2 + z_3, \\
\Delta_1 &= a_0 + a_1 + a_2, \\
\Delta_2 &= b_0 + b_1 + b_2.
\end{aligned} \tag{11}$$

By replacing Eq. (11) in Eq. (10), it is possible for us to construct the analytical solution by taking advantage of the method of undetermined coefficients.

Initially, the linearized equations of motion are

$$\begin{aligned}
x_1'' - 2y_1' - (1 + 2c_2)x_1 &= 0, \\
y_1'' + 2x_1' - (1 - c_2 + a_0)y_1 &= 0, \\
z_1'' + (c_2 - b_0)z_1 &= 0.
\end{aligned} \tag{12}$$

By solving Eq. (12), it is not difficult to obtain the first-order solution of M2N1 ME-Halo orbit as follows⁴:

$$x_1 = \alpha \cos 2f, \quad y_1 = \kappa \alpha \sin 2f, \quad z_1 = \beta \cos 2f, \quad (13)$$

where α and β are referred to as the in-plane and out-of-plane amplitudes, and κ is

$$\kappa = -\frac{1}{4} (5 + 2c_2). \quad (14)$$

Replacing Eq. (13) in Eq. (12), we can obtain the zero-order coefficients of correction terms, given by

$$a_0 = -\frac{9 + c_2(5 - 2c_2)}{5 + 2c_2}, \quad b_0 = c_2 - 4. \quad (15)$$

Notice that, for a certain system with given mass parameter μ , the coefficients a_0 , b_0 , and κ are constants. At the first order, we can get $\Delta_1 = a_0 \neq 0$ and $\Delta_2 = b_0 \neq 0$, showing that there is no linear solution for ME-Halo orbits⁵.

Then, at the second order, the equations of motion are

$$\begin{aligned} x_2'' - 2y_2' - (1 + 2c_2)x_2 &= C_{x0}^{(2)} + C_{x1}^{(2)} \cos f + C_{x3}^{(2)} \cos 3f + C_{x4}^{(2)} \cos 4f, \\ y_2'' + 2x_2' - (1 - c_2 + a_0)y_2 &= S_{y1}^{(2)} \sin f + a_1 \kappa \alpha \sin 2f + S_{y3}^{(2)} \sin 3f + S_{y4}^{(2)} \sin 4f, \\ z_2'' + (c_2 - b_0)z_2 &= C_{z0}^{(2)} + C_{z1}^{(2)} \cos f + b_1 \beta \cos 2f + C_{z3}^{(2)} \cos 3f + C_{z4}^{(2)} \cos 4f, \end{aligned} \quad (16)$$

where the expressions of $C_*^{(2)}$ and $S_*^{(2)}$ are provided by Eq. (A1) in the Appendix. The second-order analytical solution can be written as

$$\begin{aligned} x_2 &= x_{20} + x_{21} \cos f + x_{22} \cos 2f + x_{23} \cos 3f + x_{24} \cos 4f, \\ y_2 &= y_{20} + y_{21} \sin f + y_{22} \sin 2f + y_{23} \sin 3f + y_{24} \sin 4f, \\ z_2 &= z_{20} + z_{21} \cos f + z_{22} \cos 2f + z_{23} \cos 3f + z_{24} \cos 4f. \end{aligned} \quad (17)$$

Replacing Eq. (17) in Eq. (16), we can determine the second-order coordinate coefficients (x_2, y_2, z_2) and the first-order coefficients of correction terms (a_1, b_1) . It should be noted that when solving for x_{22} , y_{22} , and a_1 , the number of unknowns exceeds the number of equations. Without loss of generality, this issue can be resolved by setting $x_{22} = 0$. Similar treatment can be found in Richardson (1980). As a result, the first-order coefficients of correction terms are

$$a_1 = 0, \quad b_1 = 0, \quad (18)$$

⁴As for the M2N1 ME-Halo orbit, the in-plane and out-of-plane motion frequencies are fixed at $\omega = \nu = 2n$, where the forced frequency is $n = 1$ in normalized units.

⁵This is in agreement with Halo orbits in the CRTBP (Richardson 1980).

and those second-order non-zero coefficients of coordinates are

$$\begin{aligned}
x_{20} &= -\frac{C_{x0}^{(2)}}{(1+2c_2)}, \quad x_{21} = -\frac{(6c_2-1)C_{x1}^{(2)} + 2(5+2c_2)S_{y1}^{(2)}}{6(3+3c_2+2c_2^2)}, \\
x_{23} &= -\frac{(41+10c_2)C_{x3}^{(2)} - 6(5+2c_2)S_{y3}^{(2)}}{10(23+11c_2+2c_2^2)}, \quad x_{24} = -\frac{(19+6c_2)C_{x4}^{(2)} - 2(5+2c_2)S_{y4}^{(2)}}{3(9+2c_2)^2}, \\
y_{21} &= \frac{(5+2c_2)C_{x1}^{(2)} - (5+7c_2+2c_2^2)S_{y1}^{(2)}}{3(3+3c_2+2c_2^2)}, \\
y_{23} &= -\frac{-3(5+2c_2)C_{x3}^{(2)} + (25+15c_2+2c_2^2)S_{y3}^{(2)}}{5(23+11c_2+2c_2^2)}, \\
y_{24} &= \frac{-8(5+2c_2)C_{x4}^{(2)} + (85+44c_2+4c_2^2)S_{y4}^{(2)}}{12(9+2c_2)^2}, \\
z_{20} &= \frac{C_{z0}^{(2)}}{4}, \quad z_{21} = \frac{C_{z1}^{(2)}}{3}, \quad z_{23} = -\frac{C_{z3}^{(2)}}{5}, \quad z_{24} = -\frac{C_{z4}^{(2)}}{12}.
\end{aligned} \tag{19}$$

At last, the equations of motion for the third-order terms are

$$\begin{aligned}
x_3'' - 2y_3' - (1+2c_2)x_3 &= C_{x0}^{(3)} + C_{x1}^{(3)} \cos f + C_{x2}^{(3)} \cos 2f + C_{x3}^{(3)} \cos 3f \\
&\quad + C_{x4}^{(3)} \cos 4f + C_{x5}^{(3)} \cos 5f + C_{x6}^{(3)} \cos 6f, \\
y_3'' + 2x_3' - (1-c_2)y_3 - a_0y_3 - a_2y_1 &= S_{y1}^{(3)} \sin f + (S_{y2}^{(3)} + a_2\kappa\alpha) \sin 2f \\
&\quad + S_{y3}^{(3)} \sin 3f + S_{y4}^{(3)} \sin 4f + S_{y5}^{(3)} \sin 5f + S_{y6}^{(3)} \sin 6f, \\
z_3'' + c_2z_3 - b_0z_3 - b_2z_1 &= C_{z0}^{(3)} + C_{z1}^{(3)} \cos f + (C_{z2}^{(3)} + b_2\beta) \cos 2f \\
&\quad + C_{z3}^{(3)} \cos 3f + C_{z4}^{(3)} \cos 4f + C_{z5}^{(3)} \cos 5f + C_{z6}^{(3)} \cos 6f,
\end{aligned} \tag{20}$$

where the expressions of $C_*^{(3)}$ and $S_*^{(3)}$ are provided by Eqs. (A2) and (A3) in the Appendix. Similarly, the third-order solution can be expressed as

$$\begin{aligned}
x_3 &= x_{30} + x_{31} \cos f + x_{32} \cos 2f + x_{33} \cos 3f + x_{34} \cos 4f + x_{35} \cos 5f + x_{36} \cos 6f, \\
y_3 &= y_{30} + y_{31} \sin f + y_{32} \sin 2f + y_{33} \sin 3f + y_{34} \sin 4f + y_{35} \sin 5f + y_{36} \sin 6f, \\
z_3 &= z_{30} + z_{31} \cos f + z_{32} \cos 2f + z_{33} \cos 3f + z_{34} \cos 4f + z_{35} \cos 5f + z_{36} \cos 6f.
\end{aligned} \tag{21}$$

During the determination of (x_{32}, y_{32}, z_{32}) and (a_2, b_2) , a rank-deficiency problem arises. This is a common issue in the process of L-P method. To resolve this problem, we follow the standard treatment adopted in the analytic construction of Halo orbits (Richardson 1980; Jorba and Masdemont 1999) and eliminate the indeterminacy by setting $y_{32} = 0$ and $z_{32} = 0$, thereby ensuring the system of equations becomes solvable.

As a result, the second-order coefficients of correction terms are

$$a_2 = \frac{4C_{x2}^{(3)} - (5 + 2c_2)S_{y2}^{(3)}}{(5 + 2c_2)\kappa\alpha}, \quad b_2 = \frac{1}{\beta}C_{z2}^{(3)}, \quad (22)$$

and those third-order non-zero coefficients of coordinates are given by

$$\begin{aligned} x_{30} &= -\frac{C_{x0}^{(3)}}{1 + 2c_2}, \quad x_{31} = -\frac{(-1 + 6c_2)C_{x1}^{(3)} + 2(5 + 2c_2)S_{y1}^{(3)}}{6(3 + 3c_2 + 2c_2^2)}, \\ x_{32} &= -\frac{C_{x2}^{(3)}}{5 + 2c_2}, \quad x_{33} = -\frac{(41 + 10c_2)C_{x3}^{(3)} - (30 + 12c_2)S_{y3}^{(3)}}{10(23 + 11c_2 + 2c_2^2)}, \\ x_{34} &= -\frac{(19 + 6c_2)C_{x4}^{(3)} - 2(5 + 2c_2)S_{y4}^{(3)}}{3(9 + 2c_2)^2}, \\ x_{35} &= -\frac{(121 + 42c_2)C_{x5}^{(3)} - 10(5 + 2c_2)S_{y5}^{(3)}}{42(63 + 27c_2 + 2c_2^2)}, \\ x_{36} &= -\frac{4(11 + 4c_2)C_{x6}^{(3)} - 3(5 + 2c_2)S_{y6}^{(3)}}{8(181 + 76c_2 + 4c_2^2)}, \\ y_{31} &= -\frac{(5 + 2c_2)C_{x1}^{(3)} - (5 + 7c_2 + 2c_2^2)S_{y1}^{(3)}}{3(3 + 3c_2 + 2c_2^2)}, \\ y_{33} &= -\frac{-(15 + 6c_2)C_{x3}^{(3)} + (25 + 15c_2 + 2c_2^2)S_{y3}^{(3)}}{5(23 + 11c_2 + 2c_2^2)}, \\ y_{34} &= -\frac{-8(5 + 2c_2)C_{x4}^{(3)} + (85 + 44c_2 + 4c_2^2)S_{y4}^{(3)}}{12(9 + 2c_2)^2}, \\ y_{35} &= -\frac{-5(5 + 2c_2)C_{x5}^{(3)} + (65 + 31c_2 + 2c_2^2)S_{y5}^{(3)}}{21(63 + 27c_2 + 2c_2^2)}, \\ y_{36} &= -\frac{-12(5 + 2c_2)C_{x6}^{(3)} + (185 + 84c_2 + 4c_2^2)S_{y6}^{(3)}}{32(181 + 76c_2 + 4c_2^2)}, \\ z_{30} &= -\frac{1}{4}C_{z0}^{(3)}, \quad z_{31} = \frac{1}{3}C_{z1}^{(3)}, \quad z_{33} = -\frac{1}{5}C_{z3}^{(3)}, \quad z_{34} = -\frac{1}{12}C_{z4}^{(3)}, \\ z_{35} &= -\frac{1}{21}C_{z5}^{(3)}, \quad z_{36} = -\frac{1}{32}C_{z6}^{(3)}. \end{aligned} \quad (23)$$

In summary, the third-order expansion of M2N1 ME-Halo orbits can be organized as

$$\begin{aligned}
x &= x_{20} + x_{30} + (x_{21} + x_{31}) \cos f + (\alpha + x_{32}) \cos 2f + (x_{23} + x_{33}) \cos 3f \\
&\quad + (x_{24} + x_{34}) \cos 4f + x_{35} \cos 5f + x_{36} \cos 6f, \\
y &= y_{20} + y_{30} + (y_{21} + y_{31}) \sin f + \kappa \alpha \sin 2f + (y_{23} + y_{33}) \sin 3f \\
&\quad + (y_{24} + y_{34}) \sin 4f + y_{35} \sin 5f + y_{36} \sin 6f, \\
z &= z_{20} + z_{30} + (z_{21} + z_{31}) \cos f + \beta \cos 2f + (z_{23} + z_{33}) \cos 3f \\
&\quad + (z_{24} + z_{34}) \cos 4f + z_{35} \cos 5f + z_{36} \cos 6f,
\end{aligned} \tag{24}$$

and the correction terms can be expressed as

$$\Delta_1 = a_0 + a_2 = 0, \quad \Delta_2 = b_0 + b_2 = 0, \tag{25}$$

where $a_1 = b_1 = 0$ is considered. Considering the explicit expressions of a_2 and b_2 , we can further arrange the correction terms as follows:

$$\begin{aligned}
\Delta_1 &= a_0 + a_{200}e^2 + a_{020}\alpha^2 + a_{002}\beta^2 = 0, \\
\Delta_2 &= b_0 + b_{200}e^2 + b_{020}\alpha^2 + b_{002}\beta^2 = 0,
\end{aligned} \tag{26}$$

where the coefficients a_{200} , a_{020} , a_{002} , b_{200} , b_{020} , and b_{002} are provided by Eq. (A4) in the Appendix. The constraints given by Eq. (26) provide implicit relationships among e , α , and β . In particular, if e is treated as an independent parameter, the amplitudes α and β can be uniquely determined by

$$\begin{aligned}
\alpha &= \sqrt{\frac{b_{002}(a_0 + a_{200}e^2) - a_{002}(b_0 + b_{200}e^2)}{-a_{020}b_{002} + a_{002}b_{020}}}, \\
\beta &= \sqrt{\frac{-b_{020}(a_0 + a_{200}e^2) + a_{020}(b_0 + b_{200}e^2)}{-a_{020}b_{002} + a_{002}b_{020}}}.
\end{aligned} \tag{27}$$

3.3 High-order analytical solution

Here we extend to higher-order series expansions of ME-Halo orbits in the ERTBP. Due to the perturbations introduced by nonlinear terms, the general solution of ME-Halo orbits near the collinear libration points in the ERTBP can be expanded as a power series in terms of the eccentricity e , the in-plane amplitude α , and the out-of-plane amplitude β in the following manner:

$$\begin{aligned}
x &= \sum x_{ijk}^l e^i \alpha^j \beta^k \cos(lf), \\
y &= \sum y_{ijk}^l e^i \alpha^j \beta^k \sin(lf), \\
z &= \sum z_{ijk}^l e^i \alpha^j \beta^k \cos(lf).
\end{aligned} \tag{28}$$

Table 1 Summary of unknown terms for the n -th order solution.

$\Delta_1 y$	$\Delta_2 z$	x, y, z	x', y'	x'', y'', z''
$a_{000} y_{ijk}^l$ $a_{ij-1k} \kappa \delta_{2l}$	$b_{000} z_{ijk}^l$ $b_{ijk-1} \delta_{2l}$	$x_{ijk}^l, y_{ijk}^l, z_{ijk}^l$	$l x_{ijk}^l, l y_{ijk}^l, l z_{ijk}^l$	$l^2 x_{ijk}^l, l^2 y_{ijk}^l, l^2 z_{ijk}^l$

At the same time, the correction terms Δ_1 and Δ_2 are expanded as power series in terms of the eccentricity and amplitudes in the following form:

$$\Delta_1 = \sum a_{ijk} e^i \alpha^j \beta^k, \quad \Delta_2 = \sum b_{ijk} e^i \alpha^j \beta^k. \quad (29)$$

Here, $i, j, k \in \mathbb{N}$, $l \in \mathbb{Z}$, and l has the same parity as i . The unknown coefficients $(x_{ijk}^l, y_{ijk}^l, z_{ijk}^l, a_{ijk}^l, b_{ijk}^l)$ are iteratively determined using the perturbation method. For convenience, we introduce two orders: the order N_1 is defined in terms of the orbital eccentricity, and N_2 is the order with respect to the amplitudes α or β . The total order of the analytical solution is $N = N_1 + N_2$. For any combination of indices i, j, k, l , the conditions $0 \leq i \leq N_1$, $0 \leq j + k \leq N_2$ should be satisfied. For M2N1 ME-Halo orbits, the allowable range of l is $-i - 2(j + k) \leq l \leq i + 2(j + k)$. Considering the symmetry properties of cosine and sine functions, it is enough to compute the terms with $0 \leq l \leq i + 2(j + k)$.

As for the linear solution, the associated order is denoted as $(n_1 = 0, n_2 = 1)$, corresponding to zeroth-order in eccentricity and first-order in amplitudes. Thus, the coefficients of the first-order solution can be further expressed as

$$x_{010}^2 = 1, \quad y_{010}^2 = \kappa, \quad z_{001}^2 = 1, \quad a_{000} = -\frac{9 + c_2(5 - 2c_2)}{5 + 2c_2}, \quad b_{000} = c_2 - 4.$$

In the process of constructing higher-order solutions, it is necessary to distinguish the known terms from those unknown terms in the equations of motion. The known terms at order (n_1, n_2) arise from the right-hand side of the equations of motion, excluding the correction terms. All the known terms are collected on the right-hand side and denoted as X_{ijk}^l , Y_{ijk}^l , and Z_{ijk}^l . The unknowns at order (n_1, n_2) include the coordinate coefficients $(x_{ijk}^l, y_{ijk}^l, z_{ijk}^l)$ of the same order, and the correction-related coefficients (a_{ijk}, b_{ijk}) of order $(n_1, n_2 - 1)$. For convenience, the unknown terms of analytical solution at order (n_1, n_2) are summarized in Table 1.

Application of perturbation method indicates that those terms of the same order on both sides must be equal, allowing us to formulate the system of linear equations at order (n_1, n_2) as follows:

$$\begin{aligned} -(l^2 + 1 + 2c_2)x_{ijk}^l - 2ly_{ijk}^l &= X_{ijk}^l, \\ -(l^2 + 1 - c_2 + a_{000})y_{ijk}^l - 2lx_{ijk}^l - a_{ij-1k} \kappa \delta_{2l} &= Y_{ijk}^l, \\ (-l^2 + c_2 - b_{000})z_{ijk}^l - b_{ijk-1} \delta_{2l} &= Z_{ijk}^l, \end{aligned} \quad (30)$$

where δ_{ij} is the Kronecker symbol, with $\delta_{ij} = 1$ if $i = j$, and $\delta_{ij} = 0$ otherwise. The unknown coefficients including $(x_{ijk}^l, y_{ijk}^l, z_{ijk}^l)$ and (a_{ij-1k}, b_{ijk-1}) can be determined

by solving the linear system of equations in the cases of $l = 2$ and $l \neq 2$. See Table 2 for the coefficients of series expansions up to order 3 about the M2N1 ME-Halo orbits around L_2 in the system of $\mu = 0.0001$.

Table 2 Coefficients of correction terms and coordinates of the third-order series expansion of M2N1 ME-Halo orbits around L_2 in the dynamical model of $\mu = 0.0001$.

i	j	k		a_{ijk}	b_{ijk}
i	j	k	l	x_{ijk}^l or z_{ijk}^l	y_{ijk}^l
0	0	0		.815473465266E - 01	-.185347359371E + 00
0	0	2		.806857647185E + 00	-.535380180484E + 00
0	2	0		-.425982982820E + 01	.804332948695E + 01
2	0	0		.897012913088E + 00	.114325067073E + 01
0	0	1	2	.100000000000E + 01	
0	1	0	2	.100000000000E + 01	-.315732632031E + 01
0	0	2	0	-.255082536862E + 00	
0	0	2	4	-.111141395671E + 00	.670187851100E - 01
0	1	1	4	-.366864180416E + 00	
1	0	1	1	.469108773438E + 00	
1	1	0	3	.509046867362E - 02	.704151869059E + 00
1	1	0	1	.790992345009E + 00	-.165102706230E + 01
0	0	3	6	-.187785890778E - 01	
0	1	2	2	.370681934798E - 01	
0	1	2	6	.865444702303E - 01	.169450480988E - 01
0	2	1	6	.401585394226E + 00	
0	3	0	2	.110077910069E + 01	
0	3	0	6	-.788114962028E + 00	-.848345233831E + 00
1	0	2	1	-.692012517163E - 01	-.798581043538E - 01
1	0	2	3	-.113912738869E + 00	.940113342615E - 01
1	0	2	5	.652929569041E - 01	-.335586474518E - 01
1	1	1	1	.100871431754E + 01	
1	1	1	3	-.565989773830E + 00	
1	1	1	5	.187342231102E + 00	
1	2	0	1	-.461663256351E + 00	-.853250204681E + 00
1	2	0	3	.883266646720E + 00	.847119291068E + 00
1	2	0	5	-.487462337750E + 00	-.260887486736E + 00
2	0	1	0	-.108685090518E - 01	
2	0	1	4	.916480528772E - 01	
2	1	0	0	.145496172504E + 00	.372615077613E - 01
2	1	0	2	-.696658926851E - 01	
2	1	0	4	-.100029035334E - 01	-.236124768923E + 00

It is worth noting that ME-Halo orbits must satisfy the following correction conditions:

$$\Delta_1(e, \alpha, \beta) = 0, \quad \Delta_2(e, \alpha, \beta) = 0, \quad (31)$$

which indicate that, among the eccentricity e , and amplitudes α and β , only one is independent. Given one of these parameters, the remaining ones can be determined from Eq. (31).

4 Results

The high-order analytical solution of ME-Halo orbits in the ERTBP has been implemented in the previous section. Simulation results are presented in this section, and all results are shown in the synodic coordinate system with origin at the libration point L_2 .

4.1 Accuracy analysis

To verify the accuracy of the analytical solutions, the method of numerical integration is employed. Initially, the analytical solution of ME-Halo orbits at different orders are taken to produce initial conditions. Then, the equations of motion are numerically integrated by the RKF78 integrator. The top panels of Fig. 1 shows a comparison between analytical and numerical orbits. It shows that the analytical orbit produced from the 15th-order expansion has a better agreement with the corresponding numerically propagated orbit than the 5th-order version.

To quantitatively assess the accuracy of analytical expansions, the Euclidean norm of the position difference between analytical and numerical orbits is evaluated at a quarter period. The position deviation Δr is taken as an index of accuracy (Lei et al. 2013; Lei and Xu 2014). The bottom panels of Fig. 1 illustrates how the position deviation Δr changes with eccentricity e and the out-of-plane amplitude β for the 5th- and 15th-order analytical expansions. It is observed that a higher-order expansion holds a higher-level accuracy. In general, the error decreases with the out-of-plane amplitude β and increases with the eccentricity of primaries e .

Table 3 lists the values of e , α and Δr for varying μ , with β fixed at 0.04. The results indicate that Δr increases monotonically with μ . For systems with $\mu < 0.0001$, the deviation remains on the order of 10^{-5} , whereas as μ approaching 0.001, it grows up to the order of 10^{-3} . This is because a higher μ holds a larger ME halo orbit, as shown in Fig. 2.

Table 3 Values of e , α and Δr with β fixed at 0.04. The position deviation Δr is evaluated at a quarter period of the corresponding ME-Halo orbit.

μ	e	α	$\Delta r(\gamma_2)$
0.00008	0.070892	0.146131	2.953167E-05
0.0001	0.124957	0.146461	9.169962E-05
0.0003	0.280288	0.148482	4.751369E-04
0.0005	0.338801	0.149693	7.114512E-04
0.001	0.414768	0.151685	1.115248E-03
0.0122	0.683231	0.163858	4.888446E-03

4.2 Characteristic curves of ME-Halo orbits

As for analytical solution of ME-Halo orbits, the parameters include the mass ratio μ , the eccentricity e , the in-plane amplitude α , and the out-of-plane amplitude β . Fig. 2 illustrates the relationship among e , α , and β , corresponding to characteristic curves of ME-Halo orbits under different dynamical models specified by μ . It is observed that the mass parameter μ determines the distribution of characteristic curve of ME-Halo orbits. In particular, a lower value of μ corresponds to a smaller range of e and α (or β), while higher value of μ corresponds to a larger range of e and α (or β).

Figs. 3 and 4 present the projections of analytical M2N1 ME-Halo orbits to coordinate planes for the ERTBPs of $\mu = 0.0001$ and $\mu = 0.0005$, as the out-of-plane amplitude β varies from 0.04 to 0.2 with step of 0.04. Their locations on the characteristic curves are marked by red crosses in Fig. 2. As β increases (from the left to the

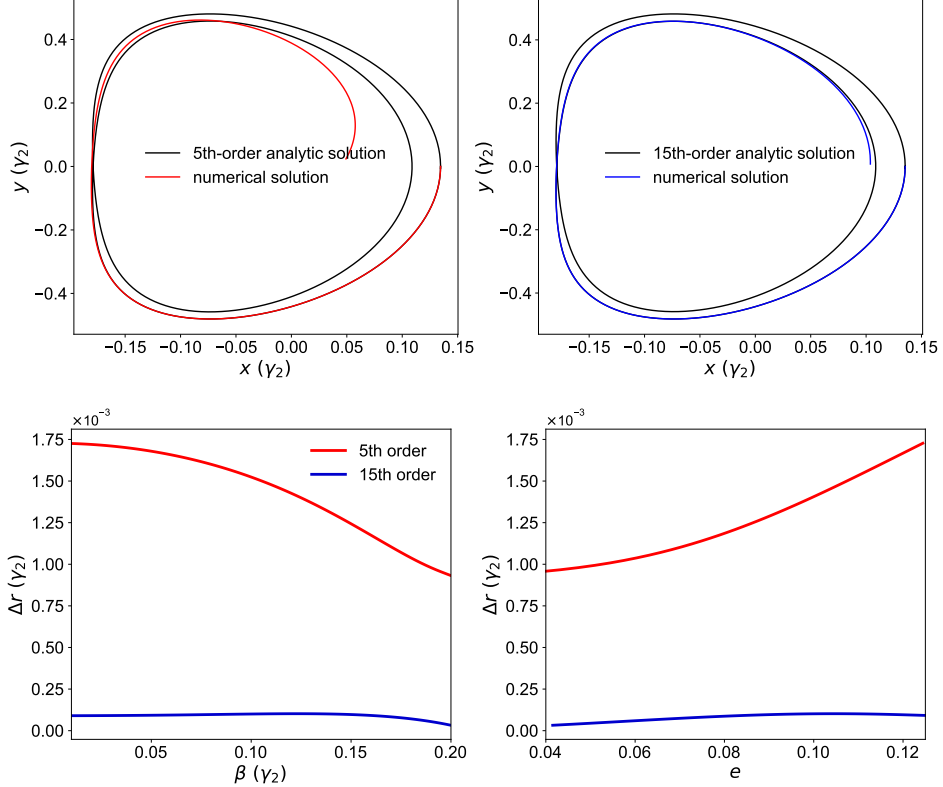


Fig. 1 Analytical ME-Halo orbits together with the associated numerically propagated orbits (*top panels*), and position deviation between analytical and numerical orbits evaluated at a quarter period (*bottom panels*). Analytical expansions up to order $n = 5$ and $n = 15$ are considered under the dynamical model of $\mu = 0.0001$. In the top panels, the out-of-plane amplitude is fixed at $\beta = 0.1$, and it holds $(e, \alpha) = (0.109232, 0.149158)$ for $n = 5$ and $(e, \alpha) = (0.112684, 0.149471)$ for $n = 15$.

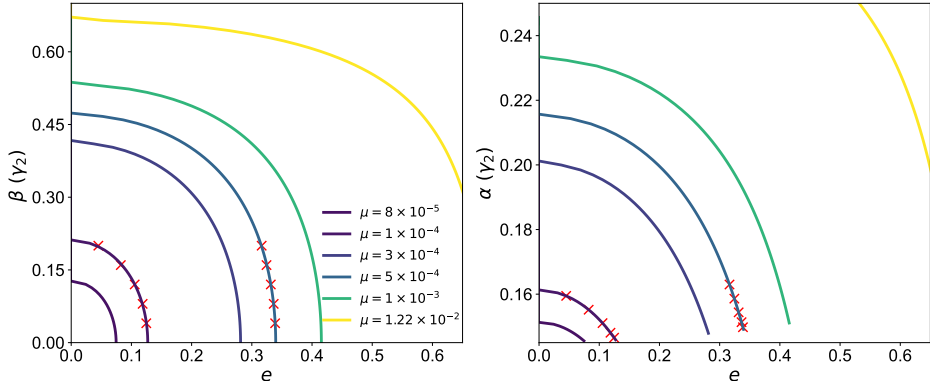


Fig. 2 Characteristic curves of the M2N1 ME-Halo orbits produced by means of 15th-order series expansions in dynamical models with different μ . The ME-Halo orbits marked by red crosses are to be presented in Figs. 3 and 4.

right), the amplitude of motion in the z direction gradually increases, causing the orbits projected onto the x - z and y - z planes to expand. On the other hand, the eccentricity e decreases with β , which results in the two loops of the orbits projected onto the x - y and y - z planes moving closer together.

The Halo orbit is symmetric with respect to the xy -plane, thus there exist two families of solutions: the northern family with $z > 0$ and the southern family with $z < 0$. Based on their initial positions, ME-Halo orbits can also be categorized into the periapsis group, which starts from the periapsis of the primary (i.e., $f_0 = 0$), and into

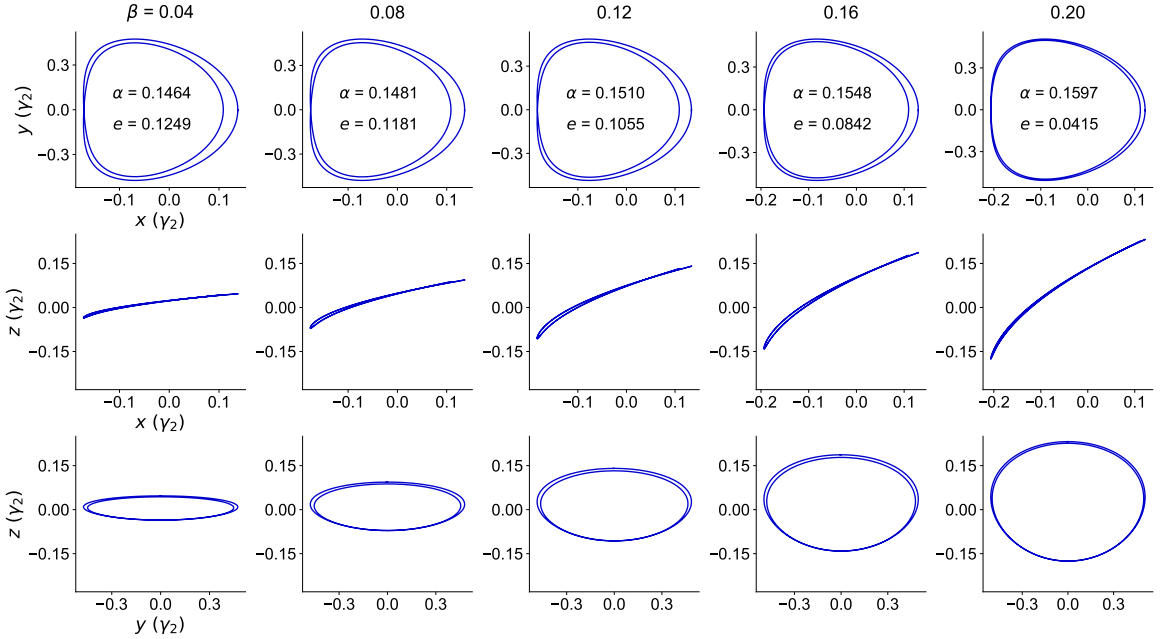


Fig. 3 Analytical M2N1 ME-Halo orbits in the northern periapsis group, shown in different coordinate planes as β changes from 0.04 to 0.2 in the dynamical model of $\mu = 0.0001$. The parameters of ME-Halo orbits, including e , α and β , are provided in the top-row panels (please see Fig. 2 for their location on the characteristic curve).

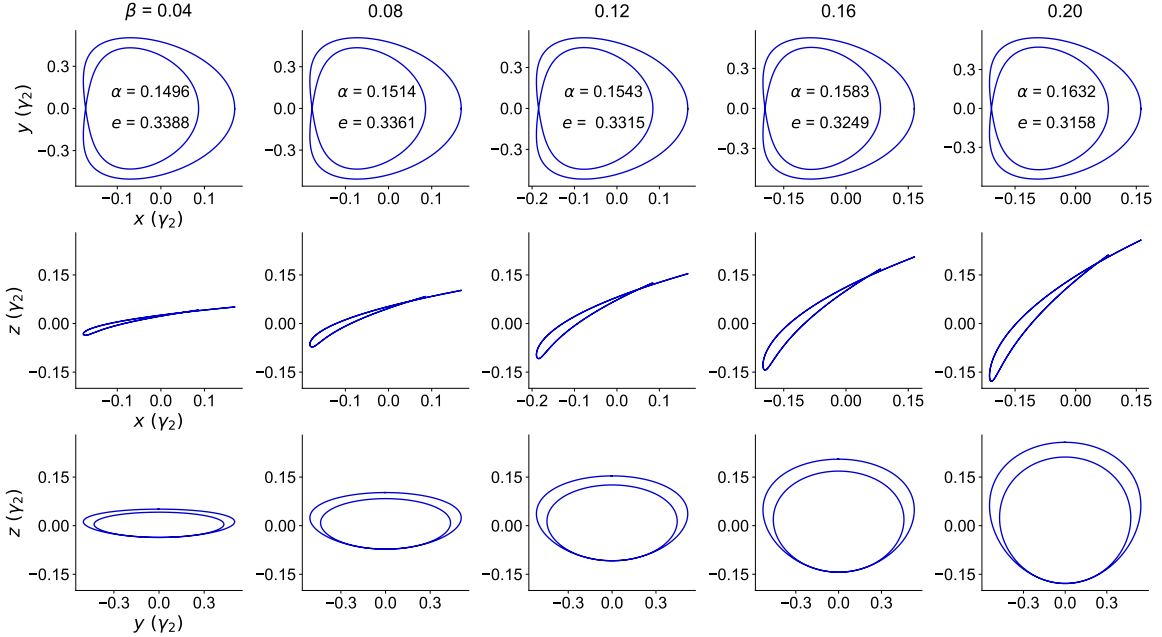


Fig. 4 Same as Fig. 3 but for the dynamical model of $\mu = 0.0005$.

the apoapsis group, which starts from the apoapsis (i.e., $f_0 = \pi$). Figs. 3 and 4 show ME-Halo orbits inside the northern periapsis group. The corresponding orbits inside the remaining three groups are shown in Figs. B1-B3 in Appendix B.

5 Numerically corrected orbits

A fixed-time single shooting method is taken to identify numerically corrected ME-Halo orbits, with the analytical solution as initial guesses.

5.1 Differential correction

For completeness, a brief introduction to the single shooting method is provided (Howell 1984). In the barycentric synodic frame, the state vector of Halo orbit is denoted by $\mathbf{X} = (X, Y, Z, X', Y', Z')^T$. Owing to the orbit's symmetry about the xz plane and the fact that its velocity is perpendicular to this plane, the initial state is chosen at the intersection point. Accordingly, the analytical solution provides the initial condition at $\mathbf{X}_0 = (X_0, 0, Z_0, 0, Y'_0, 0)^T$, with the set of adjustable parameters denoted by $\mathbf{Q} = (X_0, Z_0, Y'_0)^T$.

Due to the symmetry, Halo orbits will cross the xz plane again after half a period. Therefore, it is only necessary to compute the trajectory over half a period and then propagate it forward by the remaining half to obtain the complete periodic orbit. To ensure the condition of periodicity, the state at the half period must satisfy the following constraint, denoted by

$$\mathbf{F}(\mathbf{Q}) = (Y_{T/2}, X'_{T/2}, Z'_{T/2})^T = \mathbf{0}. \quad (32)$$

The Newton iteration method is employed to solve Eq. (32), and the correction process stops when the assumed tolerance is reached.

5.2 Numerically corrected orbits in the ERTBP

The 15th-order analytical solution is used to produce the analytical orbit, which serves as the initial guess. Then, the orbit is numerically refined to yield a high-accuracy periodic orbit based on the correction procedure.

To assess the applicability of the analytical solution with varying parameters, the mass ratio μ is fixed for the Sun–Jupiter and Earth–Moon systems, while the orbital eccentricity is changed. Table 4 lists the parameters (e, α, β) of the considered representative ME-Halo orbits. Analytical orbits are then taken as initial guesses for the single shooting method. The panels in the first-three rows of Figs. 5 show the M2N1 ME-Halo orbits around the L_2 point in the Sun–Jupiter, including the analytical orbits and the numerically corrected orbits. Fig. 6 corresponds to the case of Earth–Moon ERTBPs. In these plots, the black dashed lines represent the analytical orbits, and the red solid lines show the numerically corrected M2N1 ME-Halo orbits. The unit of length is the instantaneous distance between the primaries. It is observed that there is a good agreement between analytical orbits and numerically corrected orbits.

Additionally, a comparison is also made for ME-Halo orbits before and after correction in terms of the normalized error, defined by (Asano et al. 2015)

$$\text{error}(f) = \frac{\|\mathbf{X}_{\text{ana}}(f) - \mathbf{X}_{\text{num}}(f)\|}{\|\mathbf{X}_{\text{num}}(f)\|}, \quad (33)$$

where $\mathbf{X}_{\text{ana}}(f)$ and $\mathbf{X}_{\text{num}}(f)$ are the analytical and numerical orbits, respectively. Please refer to the bottom panels of Figs. 5 and 6 for the curves of $\text{error}(f)$. It is observed that even in cases with relatively large eccentricity, the constructed analytical solutions remain high-accuracy approximations for periodic orbits in the full dynamical model. For $\mu = 0.00095$, the normalized error remains below 0.05% over the entire range of

true anomaly. Similarly, for $\mu = 0.0122$, the error is also bounded within 0.5% across all values of f .

Table 4 Parameters of M2N1 ME-Halo orbits under the Sun–Jupiter and Earth–Moon models but with different primary eccentricities.

μ	e	α	β
0.00095 (S–J)	0.048400	0.231182	0.526408
	0.100000	0.229257	0.518509
	0.200000	0.220807	0.483350
	0.300000	0.202339	0.402660
0.01220 (E–M)	0.054800	0.286478	0.664588
	0.100000	0.285941	0.662558
	0.200000	0.283497	0.653372
	0.300000	0.278859	0.636102

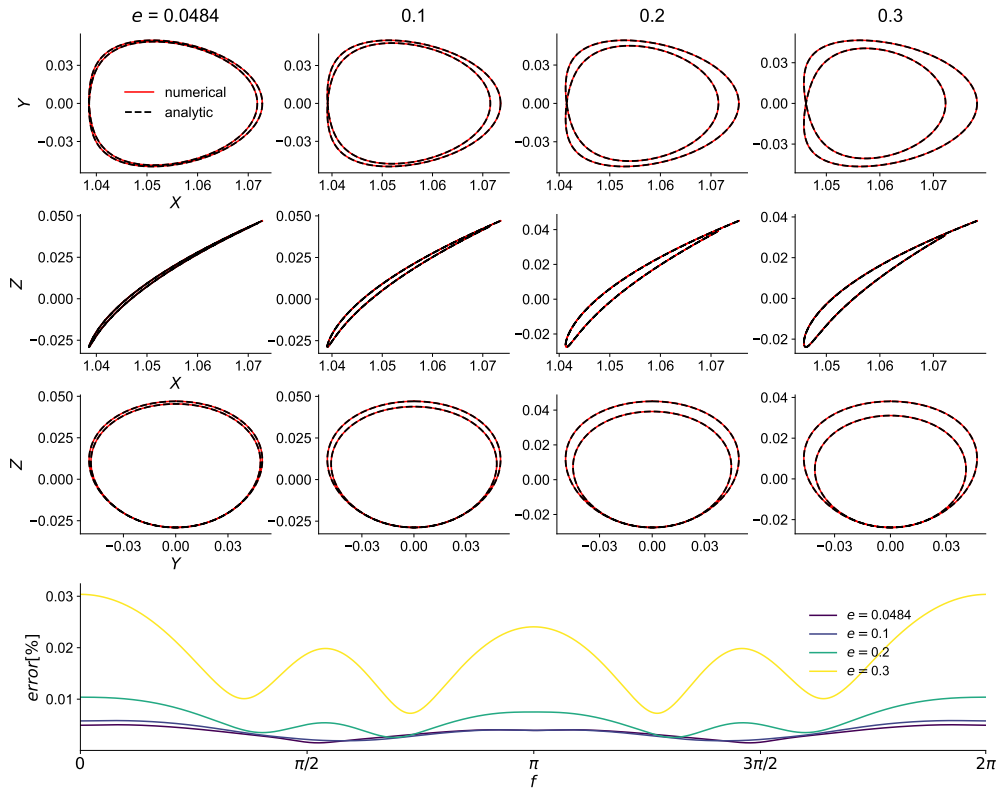


Fig. 5 The numerically corrected orbits together with the analytical M2N1 ME-Halo orbits (panels in the top three rows), and the normalized error between the analytical and numerical orbits as a function of the true anomaly (bottom row panels) in the Sun–Jupiter systems with different eccentricities.

The numerical results confirm the effectiveness of the analytical solution developed in this study under the framework of ERTBP, fully demonstrating its reliability in terms of both accuracy and applicability. This provides a robust theoretical foundation

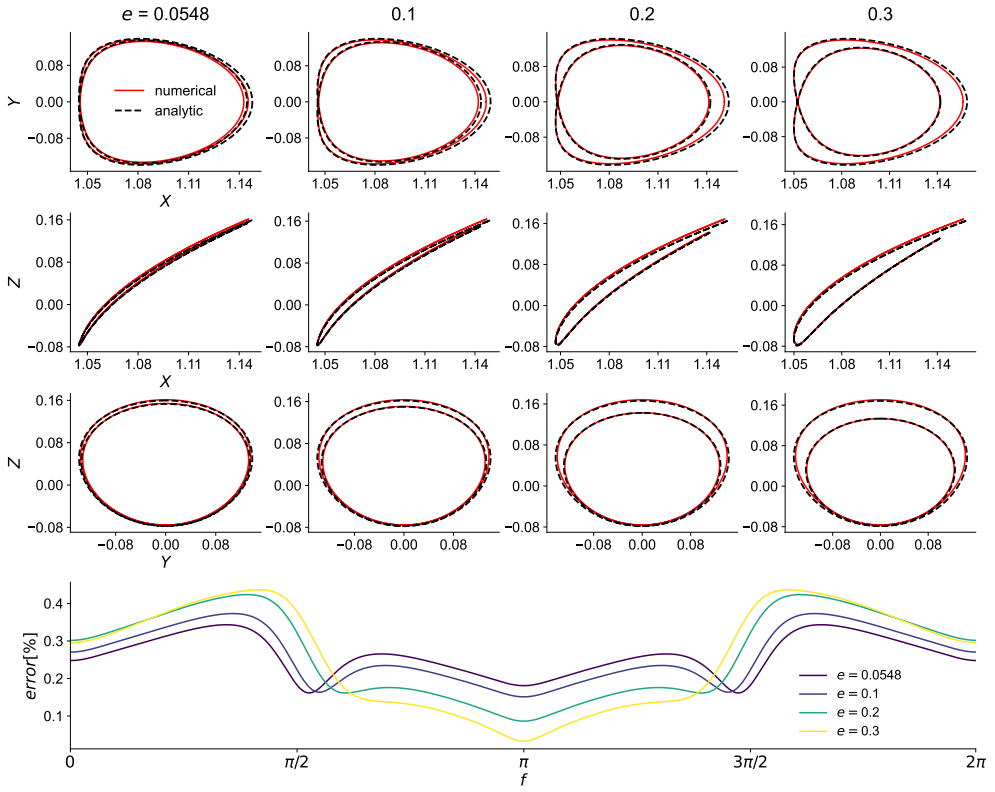


Fig. 6 Same as 5 but for the Earth–Moon system.

for its use in trajectory design for deep space exploration missions. In particular, ME-Halo orbits, serving as three-dimensional parking and transfer orbits, offer significant advantages, including low energy consumption, short orbital periods, and high transfer flexibility. These characteristics make them increasingly valuable orbital assets for missions targeting the Earth-Moon system and beyond.

6 Conclusion

In this study, we propose a novel method for constructing high-order expansions of ME-Halo orbits near collinear libration points in the framework of ERTBP. Specifically, two correction terms are introduced into the equations of motion. The first correction term, denoted by $\Delta_1 y$, is employed to enforce a specific commensurability between the forced frequency (n) and either the in-plane frequency (ω) or the out-of-plane frequency (ν). The second correction term, denoted by $\Delta_2 z$, is introduced to achieve the frequency degeneracy condition of $\omega = \nu$ (also known as the Halo orbit condition).

The perturbation method is employed to construct high-order expansions of ME-Halo orbits. In this approach, both the coordinate variables (x, y, z) and the correction terms (Δ_1, Δ_2) are expressed as power series in three parameters: the orbital eccentricity of the primary body (e), the in-plane amplitude (α), and the out-of-plane amplitude (β). For ME-Halo orbits, these parameters (e, α, β) must strictly satisfy the correction

conditions $\Delta_1(e, \alpha, \beta) = 0$ and $\Delta_2(e, \alpha, \beta) = 0$, implying that only one of them can be treated as an independent variable.

Based on the constructed analytical solution, characteristic curves of ME-Halo orbits can be derived analytically in the (e, α) and (e, β) spaces under dynamical models with different mass parameters μ . Due to the system's inherent symmetry, analytical ME-Halo orbits can be systematically categorized into four distinct groups: the southern periapsis group, the southern apoapsis group, the northern periapsis group, and the northern apoapsis group. These families of periodic orbits provide rich insights into the dynamical behavior near collinear libration points in the ERTBP.

The accuracy of the high-order expansions of ME-Halo orbits is evaluated by comparing the analytical solutions with numerically integrated orbits. The results demonstrate that higher-order expansions yield significantly improved precision. Consequently, the analytical solutions developed in this study can serve as highly accurate initial guesses for generating numerically corrected ME-Halo orbits. This capability is validated through the successful construction of numerically corrected ME-Halo orbits in both the Sun–Jupiter and Earth–Moon systems with a large range of orbital eccentricities.

Future work could further leverage the proposed analytical solution as a high-accuracy initial guess within multiple shooting methods, embedded in a high-fidelity dynamical model constructed using JPL ephemerides. By incorporating perturbative effects such as solar radiation pressure and gravitational influences from additional planetary bodies, the long-term evolution and maintenance requirements of the orbits can be systematically evaluated under realistic dynamical environments. This would enhance the practical robustness and applicability of multi-revolution targeting strategies for deep space missions.

This study focuses exclusively on M2N1 ME-Halo orbits. However, more complex resonant configurations, such as M3N1 and M5N2, are also commonly found in realistic celestial systems (Peng and Xu 2015b). These configurations exhibit richer dynamical behaviors and hold significant research interest and promising applications. Future work could extend the current methodology to encompass a broader class of resonant structures, with the goal of developing a unified high-order analytical framework capable of addressing stronger nonlinearities and more intricate resonance conditions. Such a framework would offer a more general and robust theoretical foundation for the analysis and trajectory design of ME-Halo orbits within three-body gravitational systems.

Acknowledgements. The authors wish to thank the anonymous reviewer for insightful comments, which help to improve the readability of the paper. This work is financially supported by the National Natural Science Foundation of China (Nos. 12573063 and 12233003) and the China Manned Space Program with grant no. CMS-CSST-2025-A16.

Author Contributions. Xiaoyan Leng performed the research and wrote the main manuscript. Hanlun Lei supervised the research and reviewed the manuscript.

Data availability. No datasets were generated or analyzed during the current study.

Declarations

Conflict of interest. The authors declare no conflict of interest.

Appendix A Coefficients of the equations of motion

The coefficients of the equations of motion at the second order are

$$\begin{aligned}
C_{x0}^{(2)} &= \frac{3}{4}c_3(2\alpha^2 - \beta^2 - \alpha^2\kappa^2), & C_{x1}^{(2)} &= -\frac{1}{2}(1 + 2c_2)e\alpha, \\
C_{x3}^{(2)} &= -\frac{1}{2}(1 + 2c_2)e\alpha, & C_{x4}^{(2)} &= \frac{3}{4}c_3(2\alpha^2 - \beta^2 + \alpha^2\kappa^2), \\
S_{y1}^{(2)} &= \frac{1}{2}\kappa(-1 + c_2)e\alpha, & S_{y3}^{(2)} &= \frac{1}{2}\kappa(-1 + c_2)e\alpha, & S_{y4}^{(2)} &= -\frac{3}{2}c_3\kappa\alpha^2, \\
C_{z0}^{(2)} &= -\frac{3}{2}c_3\alpha\beta, & C_{z1}^{(2)} &= \frac{1}{2}(-1 + c_2)e\beta, \\
C_{z3}^{(2)} &= \frac{1}{2}(-1 + c_2)e\beta, & C_{z4}^{(2)} &= -\frac{3}{2}c_3\alpha\beta,
\end{aligned} \tag{A1}$$

and the coefficients of the equations of motion at the third order are

$$\begin{aligned}
C_{x0}^{(3)} &= \frac{1}{4}[-2ex_{21}(1+2c_2) + e^2\alpha(1+2c_2)], \\
C_{x1}^{(3)} &= -\frac{1}{4}[6c_3(-2x_{21}\alpha - 2x_{23}\alpha + z_{21}\beta + z_{23}\beta + y_{21}\alpha\kappa + y_{23}\alpha\kappa) \\
&\quad + (4+8c_2)ex_{20} - 3ec_3(\beta^2 - 2\alpha^2 + \kappa^2\alpha^2)], \\
C_{x2}^{(3)} &= \frac{1}{2}[-e(1+2c_2)(x_{21} + x_{23}) + 3c_3(4x_{20}\alpha + 2x_{24}\alpha - 2z_{20}\beta - z_{24}\beta - y_{24}\alpha\kappa) \\
&\quad + e^2\alpha(1+2c_2) - 3c_4\alpha(3\beta^2 + \alpha^2\kappa^2 - 2\alpha^2)], \\
C_{x3}^{(3)} &= \frac{1}{8}[12c_3(2x_{21}\alpha - z_{21}\beta + y_{21}\alpha\kappa) \\
&\quad - e(4x_{24} + 8c_2x_{24} + 6c_3\alpha^2 - 3c_3\beta^2 + 3c_3\alpha^2\kappa^2)], \\
C_{x4}^{(3)} &= \frac{1}{4}(-2ex_{23} + e^2\alpha)(1+2c_2), \\
C_{x5}^{(3)} &= \frac{1}{8}[12c_3(2x_{23}\alpha - z_{23}\beta + y_{23}\alpha\kappa) - (4+8c_2)ex_{24} - 3ec_3(-\beta^2 + 2\alpha^2 + \kappa^2\alpha^2)], \\
C_{x6}^{(3)} &= \frac{1}{2}[-3c_4\alpha\beta^2 + 3c_3(2x_{24}\alpha - z_{24}\beta + y_{24}\alpha\kappa) + c_4\alpha^3(2 + 3\kappa^2)], \\
S_{y1}^{(3)} &= \frac{1}{2}[(-1 + c_2)ey_{22} + 3c_3\alpha(y_{21} - y_{23} - x_{21}\kappa + x_{23}\kappa)], \\
S_{y2}^{(3)} &= \frac{1}{8}[4e(-1 + c_2)(y_{21} + y_{23}) + 8a_2\alpha\kappa - 12\alpha c_3(y_{24} + 2x_{20}\kappa - x_{24}\kappa) \\
&\quad - 4e^2\alpha\kappa(-1 + c_2) + 3\alpha c_4\kappa(\beta^2 - 4\alpha^2 + 3\kappa^2\alpha^2)], \\
S_{y3}^{(3)} &= \frac{1}{4}[-6c_3\alpha(y_{21} + x_{21}\kappa) + 2ey_{24}(-1 + c_2) + 3c_3e\alpha^2\kappa], \\
S_{y4}^{(3)} &= \frac{1}{4}(-1 + c_2)(2ey_{23} - e^2\alpha\kappa), \\
S_{y5}^{(3)} &= \frac{1}{4}[2ey_{24}(-1 + c_2) + 3c_3e\alpha^2\kappa - 6c_3\alpha(y_{23} + x_{23}\kappa)], \\
S_{y6}^{(3)} &= -\frac{3}{8}\alpha[4c_3(y_{24} + x_{24}\kappa) + c_4\kappa(-\beta^2 + 4\alpha^2 + \alpha^2\kappa^2)],
\end{aligned} \tag{A2}$$

and

$$\begin{aligned}
C_{z0}^{(3)} &= \frac{1}{4} [2ez_{21}(-1 + c_2) + e^2\beta(1 - c_2)], \\
C_{z1}^{(3)} &= (-1 + c_2)ez_{20} + \frac{3}{2}c_3e\alpha\beta - \frac{3}{2}c_3(z_{21}\alpha + z_{23}\alpha + x_{21}\beta + x_{23}\beta), \\
C_{z2}^{(3)} &= \frac{1}{8} [4e(-1 + c_2)(z_{21} + z_{23}) - 4e^2\beta(-1 + c_2) \\
&\quad - 12c_3(2\alpha z_{20} + \alpha z_{24} + 2\beta x_{20} + \beta x_{24}) + \beta(8b_2 + 9c_4\beta^2 - 36c_4\alpha^2 + 3c_4\alpha^2\kappa^2)], \\
C_{z3}^{(3)} &= \frac{1}{4} [2ez_{24}(-1 + c_2) + 3c_3e\alpha\beta - 6c_3(z_{21}\alpha + x_{21}\beta)], \\
C_{z4}^{(3)} &= \frac{1}{4}(2ez_{23} - e^2\beta)(1 - c_2), \\
C_{z5}^{(3)} &= \frac{1}{4} [2(-1 + c_2)ez_{24} + 3c_3e\alpha\beta - 6c_3(z_{23}\alpha + x_{23}\beta)], \\
C_{z6}^{(3)} &= -\frac{3}{8} [-c_4\beta^3 + 4c_3(z_{24}\alpha + x_{24}\beta) + c_4\alpha^2\beta(4 + \kappa^2)]. \tag{A3}
\end{aligned}$$

The coefficients of correction terms associated with the third-order analytical solution are given by

$$\begin{aligned}
a_{200} &= \frac{1}{30(5 + 2c_2)^2(3 + 3c_2 + 2c_2^2)(23 + 11c_2 + 2c_2^2)} [-54594 - 104625c_2 - 39721c_2^2 \\
&\quad + 28869c_2^3 + 29103c_2^4 + 8768c_2^5 + 1272c_2^6 + 48c_2^7 - 16c_2^8], \\
a_{020} &= \frac{3}{128(1 + 2c_2)(5 + 2c_2)^2(9 + 2c_2)^2} [c_3^2(73945 + 29900c_2 + 245916c_2^2 \\
&\quad + 208032c_2^3 + 65904c_2^4 + 9408c_2^5 + 576c_2^6) - c_4(9 + 2c_2)^2(723 + 1886c_2 \\
&\quad + 2168c_2^2 + 3056c_2^3 + 1008c_2^4 + 96c_2^5)], \\
a_{002} &= -\frac{3}{8(1 + 2c_2)(5 + 2c_2)^2(9 + 2c_2)^2} [c_3^2(7325 + 1480c_2 - 2120c_2^2 - 736c_2^3 - 48c_2^4) \\
&\quad + (9 + 2c_2)^2c_4(-167 - 314c_2 + 44c_2^2 + 8c_2^3)], \\
b_{200} &= -\frac{1}{30}(16 - 17c_2 + c_2^2), \\
b_{020} &= \frac{3}{128(1 + 2c_2)(9 + 2c_2)^2} [c_3^2(-7325 - 1480c_2 + 2120c_2^2 + 736c_2^3 + 48c_2^4) \\
&\quad - (9 + 2c_2)^2c_4(-167 - 314c_2 + 44c_2^2 + 8c_2^3)], \\
b_{002} &= \frac{3}{8} \left[\frac{(505 + 260c_2 + 36c_2^2)c_3^2}{(1 + 2c_2)(9 + 2c_2)^2} - 3c_4 \right]. \tag{A4}
\end{aligned}$$

Appendix B Multi-revolution Halo orbits in different groups

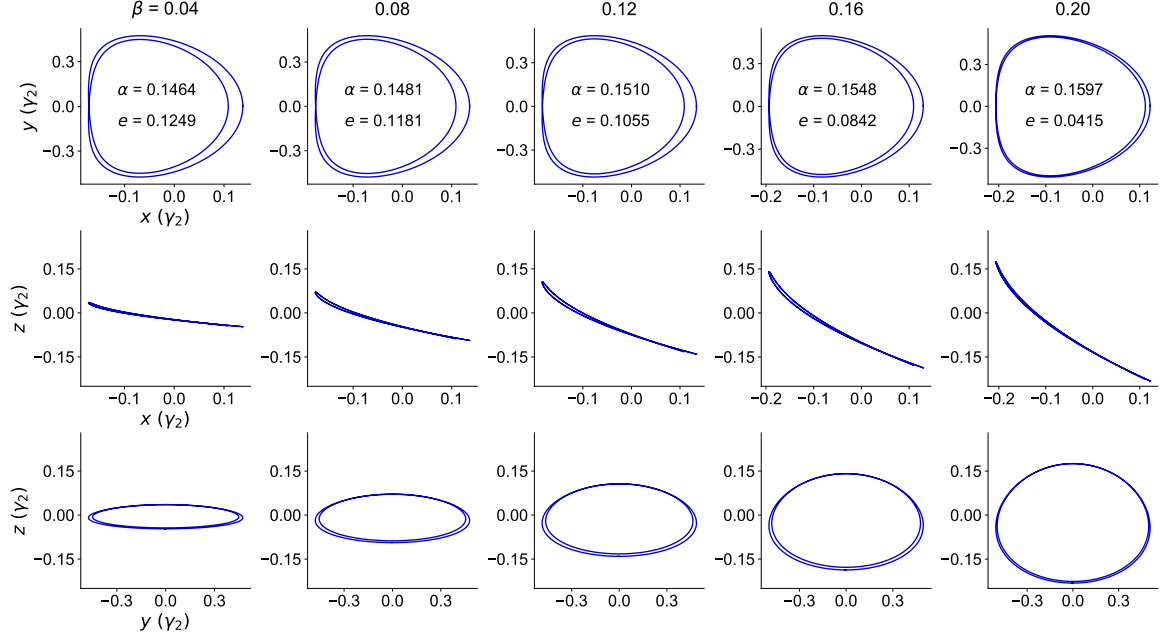


Fig. B1 Analytical M2N1 ME-Halo orbits in the southern periapsis group, shown in different coordinate planes as β varies from 0.04 to 0.2 in the dynamical model of $\mu = 0.0001$.

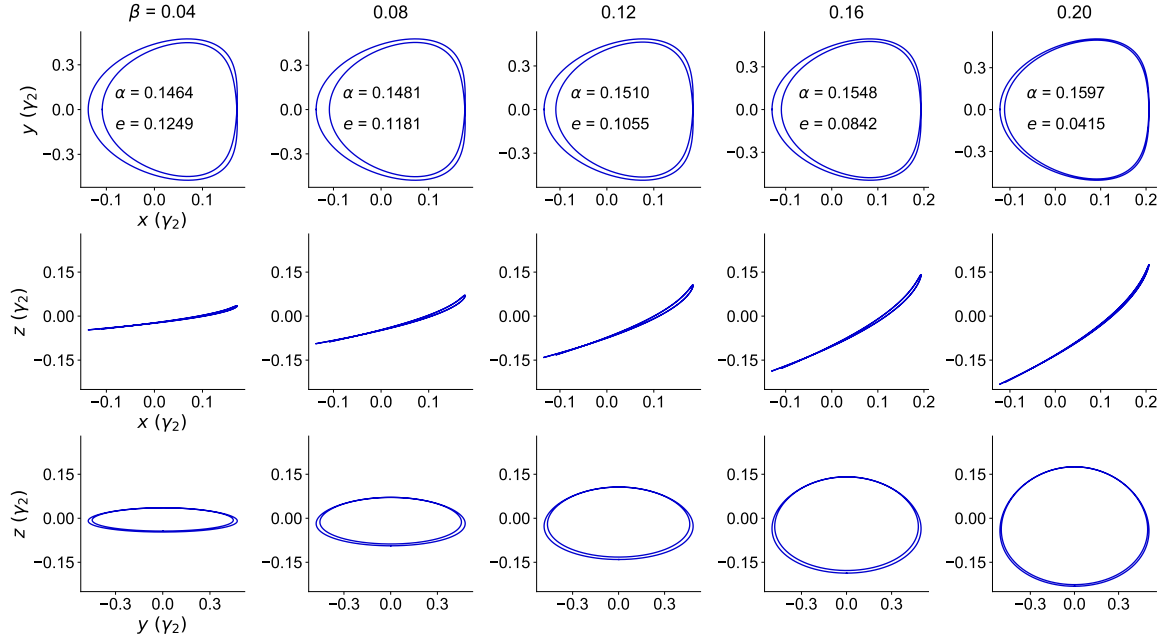


Fig. B2 Analytical M2N1 ME-Halo orbits in the northern apoapsis group, shown in different coordinate planes as β varies from 0.04 to 0.2 in the dynamical model of $\mu = 0.0001$.

References

Asano Y, Yamada K, Jikuya I (2015) Approximating elliptic halo orbits based on the variation of constants. *Acta Astronaut* 113:169–179

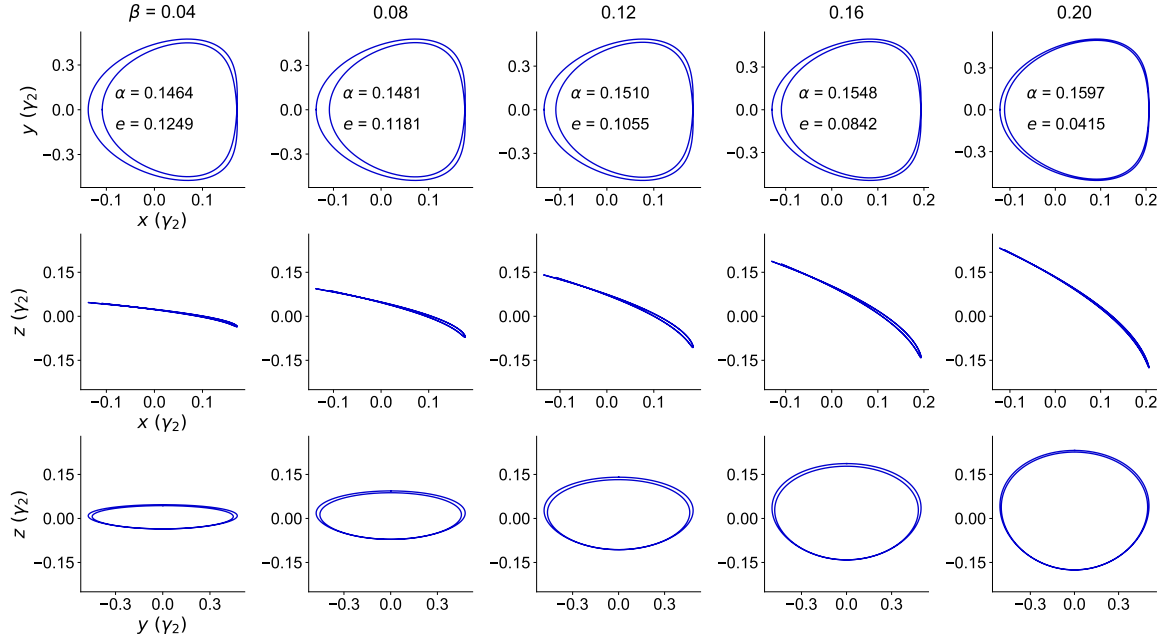


Fig. B3 Analytical M2N1 ME-Halo orbits in the southern apoapsis group, shown in different coordinate planes as β varies from 0.04 to 0.2 in the dynamical model of $\mu = 0.0001$.

Bernelli Zazzera F, Topputto F, Marchetti M (2004) Assessment of mission design including utilization of libration points and weak stability boundaries. Tech. rep., Department of Aerospace Engineering, Politecnico di Milano

Burattini C, Colombo C, Trisolini M (2024) Aerogel-based collection of ejecta material from asteroids from libration point orbits: Dynamics and capture design. *Astrodyn* 8(4):529–551

Campagnola S, Lo M, Newton P (2008) Subregions of motion and elliptic halo orbits in the elliptic restricted three-body problem. In: 18th AAS/AIAA Space Flight Mechanics Meeting, American Astronautical Society

Ceccaroni M, Celletti A, Pucacco G (2016) Halo orbits around the collinear points of the restricted three-body problem. *Physica D* 317:28–42

Celletti A, Lhotka C, Pucacco G (2024) The dynamics around the collinear points of the elliptic three-body problem: A normal form approach. *Physica D* 468:134302

Chujo T (2024) Quasi-periodic orbits of small solar sails with time-varying attitude around earth–moon libration points. *Astrodyn* 8(1):161–174

Conti M, Circi C (2025) Design of halo orbit constellation for lunar global positioning and communication services. *Astrodyn* 9(2):231–245

Farquhar R, Kamel A (1973) Quasi-periodic orbits about the translunar libration point. *Celest Mech* 7(4):458–473

Ferrari F, Lavagna M (2018) Periodic motion around libration points in the elliptic restricted three-body problem. *Nonlinear Dyn* 93:453–462

Gao C, Zhang K, Deng Z, et al (2025) Bounds of relative motion for resonant solar-sail halo orbits in earth–moon system. *Astrodyn* 9(5):807–820

Heppenheimer T (1973) Out-of-plane motion about libration points: nonlinearity and eccentricity effects. *Celest Mech* 7(2):177–194

Hou X, Liu L (2011) On motions around the collinear libration points in the elliptic restricted three-body problem. *Mon Not R Astron Soc* 415:3552–3560

Howell KC (1984) Three-dimensional, periodic, ‘halo’ orbits. *Celest Mech* 32:53–71

Huang J, Biggs JD, Cui N (2020) Families of halo orbits in the elliptic restricted three-body problem for a solar sail with reflectivity control devices. *Adv Space Res* 65:1070–1082

Jorba Á, Masdemont J (1999) Dynamics in the center manifold of the collinear points of the restricted three-body problem. *Physica D* 132:189–213

Lei H (2024) Perturbation methods and theory. Nanjing University Press, Nanjing

Lei H, Xu B (2014) High-order solutions around triangular libration points in the elliptic restricted three-body problem and applications to low energy transfers. *Commun Nonlinear Sci Numer Simul* 19:3374–3398

Lei H, Xu B, Hou X, et al (2013) High-order solutions of invariant manifolds associated with libration point orbits in the elliptic restricted three-body system. *Celest Mech Dyn Astron* 116(4):389–432

Lin M, Chiba H (2025) Bifurcation mechanism of quasi-halo orbit from lissajous orbit. *J Guid Control Dyn* 48(1):71–83

Luo T, Pucacco G, Xu M (2020) Lissajous and halo orbits in the restricted three - body problem by normalization method. *Nonlinear Dyn* 101:2629 – 2644

Masdemont J (2005) High-order expansions of invariant manifolds of libration point orbits with applications to mission design. *Dyn Syst* 20:59–113

Moulton F (1920) Periodic Orbits. Carnegie Institution of Washington, Washington

Neelakantan R, Ramanan R (2021) Design of multi-revolution orbits in the framework of elliptic restricted three-body problem using differential evolution. *J Astrophys Astron* 42(1):5

Neelakantan R, Ramanan R (2022) Two-impulse transfer to multi-revolution halo orbits in the earth–moon elliptic restricted three body problem framework. *J Astrophys*

Paez RI, Guzzo M (2022) On the semi-analytical construction of halo orbits and halo tubes in the elliptic restricted three-body problem. *Physica D* 439:133402

Parker JS, Anderson RL (2014) Low-Energy Lunar Trajectory Design, 1st edn. *JPL Deep-Space Communications and Navigation Series*, Wiley

Peng H, Bai X (2018) Natural deep space satellite constellation in the earth-moon elliptic system. *Acta Astronaut* 153:240–258

Peng H, Xu S (2015a) Low-energy transfers to a lunar multi-revolution elliptic halo orbit. *Astrophys Space Sci* 357(1):87

Peng H, Xu S (2015b) Stability of two groups of multi-revolution elliptic halo orbits in the elliptic restricted three-body problem. *Celest Mech Dyn Astron* 123:279–303

Peng H, Xu S (2015c) Transfer to a multi-revolution elliptic halo orbit in earth-moon elliptic restricted three-body problem using stable manifold. *Adv Space Res* 55:1015–1027

Peng H, Liao Y, Bai X, et al (2017) Maintenance of libration point orbit in elliptic sun–mercury model. *IEEE Trans Aero Electron Syst* 54(1):144–158

Richardson DL (1980) Analytic construction of periodic orbits about the collinear points. *Celest Mech* 22:241–253

Sanaga RR, Howell KC (2025) Leveraging the hill restricted four-body problem to investigate the ephemeris transition characteristics in the earth-moon l_2 halo orbit region. *Astrodyn* 9(5):785–805

Sarris E (1989) Families of symmetric-periodic orbits in the elliptic three-dimensional restricted three-body problem. *Astrophys Space Sci* 162(1):107–122

Servadio S, Arnas D, Linares R (2023) Dynamics near the three-body libration points via koopman operator theory. *J Guid Control Dyn* 46(5):1–36

Szebehely V (1967) Theory of Orbits - The Restricted Problem of Three Bodies. Academic Press, New York

Yamaguchi S, Hiraiwa N, Bando M, et al (2025) Trajectory design for awaiting comets on invariant manifolds with optimal control. *Astrodyn* 9(4):565–581

Zheng Y, Zhao M (2024) Universal method for designing periodic orbits by homotopy classes in the elliptic restricted three-body problem. *Astrodyn* 8(1):175–188